Application of a cellular stress transfer model for retrogressive landslides

Andrew Mitchell, Siobhan Whadcoat & Scott McDougall
Department of Earth, Ocean and Atmospheric Sciences – University of British Columbia, Vancouver, BC, Canada
Michael Porter
BGC Engineering Inc., Vancouver, British Columbia, Canada
Sarah Gaib
Ministry of Transportation and Infrastructure, Victoria, British Columbia, Canada

ABSTRACT
The upslope growth of retrogressive landslides is generally difficult to model. A cellular stress transfer model is a deterministic, numerical model that operates on a grid, and allows the patterns and underlying mechanics of movements to be explored using a reduced complexity approach. The model is time-dependent, which allows stress to transfer between cells, thereby allowing the system behaviour to be driven by spatial interactions over time. Once a cell reaches peak stress, a decrease to residual stress is simulated, and stress is transferred to surrounding cells. An initial demonstration of this model has been completed using data from Ten Mile Slide, British Columbia. The change in surface topography found through airborne LiDAR scanning change detection analysis was compared to the patterns of residual strength cells from the cellular model analysis. It was found that the model is generally able to reproduce observed patterns of slope damage and displacement.

RÉSUMÉ
La rétrogression des glissements de terrain est difficile à simuler. Un modèle cellulaire de transfert du stress est un modèle numérique et déterministique qui utilise une grille, et qui permet d'examiner l'expression et le mécanisme du mouvement au moyen d'une approche de complexité reduite. Le transfert du stress entre les cellules est fonction du temps, donc le système interagit dans l'espace et le temps. Lorsqu'une cellule atteint une valeur critique de stress, sa stress est réduite à une valeur résiduelle, et le stress est redistribué aux cellules voisines. Le modèle a été initialement déterminé avec des données obtenues à Ten Mile Slide, en Colombie Britannique. Les modifications de la topographie mesurées par analyses du changement sur la base de nuages de points de LiDAR aérienont été comparées aux cellules de résistance réduites du modèle. Le modèle est généralement capable de reproduire l'expression des fractureset les déplacements observés

1 INTRODUCTION

Potential retrogression is an important consideration when assessing future hazards for many landslide types. The patterns of movement within active landslides are also commonly observed to be variable (i.e. different regions of the slide move at different rates). In this paper, we introduce a cellular automata model as a means to assess potential retrogression and variable movement within landslides. The model uses a simplified representation of the stress state and a generalized stress reduction function that leads to stress transfer between model grid cells. An initial model demonstration is presented for a translational landslide that has developed within the body of an ancient earth flow.

1.1 Retrogressive Landslides

Many types of landslides can enlarge through headward retrogression (Hungr et al. 2014). Understanding retrogression is important when assessing landslide risks to elements upslope of a retrogressive slide. For instance, assessing areas potentially affected by retrogression, and assigning probable time frames for these effects are questions that practitioners must address. It can also be an important consideration when designing stabilization measures for a slope, as retrogression of the slide could lead to an increase in driving force that would need to be resisted by a stabilization system. Alternatively, lateral progression of a landslide could result in instabilities beyond the zone of influence of stabilization measures.

Potential retrogression can be modelled using Limit Equilibrium analysis by searching for areas where potential new critical slip surfaces could occur, however, this approach gives limited insight into how the changing stress conditions within a landslide lead to the new slip surface forming. More advanced numerical modelling, such as finite element and finite difference models, can address these questions, but they require a detailed characterization of the geotechnical properties of a landslide to confidently apply the models. Some recent examples of this approach in the literature include the use of finite element analysis to model progressive failures in both the upslope and downslope directions in sensitive clay (Dey et al. 2016), and the use of finite difference analysis to model upslope retrogression of a planar failure on a rock slope (Hu et al. 2018). A finite element approach also allows consideration of other effects, such as transient unsaturated conditions (Leshchinsky et al. 2015).

Some of the limitations of limit equilibrium analysis have been addressed to examine retrogression or progressive failures in a reduced complexity framework. Time dependent factors of safety have been calculated by considering strain softening in a limit equilibrium model (Khan et al. 2002, Tiande et al. 1999), but these methods are not commonly used in practice.

1.2 Cellular Automata Models

Cellular automata models, referred to as cellular models in this paper, are used to simulate the interactions between components of a system through space and time (Wolfram 1983). Cellular models operate as reduced complexity models on a regular grid system. The interactions between grid cells determine how the system evolves (Coulthard et al. 2007). The emergent behaviour of cellular models is not calculable from the individual model components alone but emerges from the interactions within the model. The iterative progression of a cellular model allows this emergent behaviour to be observed.

Cellular models based on concepts of self-organised criticality (Bak et al. 1988) have been used for regional scale modelling of landslide areas (Hergarten 2003, Piegari et al. 2006, Luicci et al. 2017), mass loss from near vertical glacier surfaces (Chapius and Tetzlaff, 2014), and slope scale modelling of rockfalls in near vertical cliffs (Whadcoat 2017).

Conventionally, cellular models assign a scalar property to each grid cell. The scalar property is able to change due to exogenic and/or endogenic forcing, where exogenic forcing is typically applied to the whole model and endogenic forcing is represented by the interactions between grid cells. This approach is well suited to simulating slope failures, allowing both external forces (e.g. weathering) and internal slope dynamics (e.g. fracture growth) to be considered.

1.3 Objective

The objective of the current work is to investigate a retrogressive stress transfer mechanism implemented in a cellular model at a “proof of concept” level. The model presented in this paper specifically addresses upslope retrogression within a landslide, assuming the basal shear surface is at limiting equilibrium (balanced driving and resisting forces) for each cell. The stress transfer is solely the result of material within the slide mass above the basal surface transitioning from peak to residual stress. Stress is assumed to transfer only in the upslope and lateral directions, in essence representing the arching effect resulting from a residual strength cell unable to withstand the total stress being transferred from the weight of the slope above. The current model does not represent downslope movements, thus, when a cell reaches residual stress, it does not displace downslope or increase stress on the cells downslope of it.

The simplified stress transfer assumptions do not allow a detailed examination of the specific micromechanics on an unstable slope. What this approach allows is a rapid assessment of potential retrogression when limited information on the mechanical properties of the slope are known. This approach could be applied where detailed surface topography information from remote sensing is available, such as LiDAR scanning data, and a failure surface geometry can be inferred.

2 METHODOLOGY

The slide mass is represented as a rectangular grid of cells. It is assumed that all cells are at, or are potentially at, limiting equilibrium on their base, and as a result the model does not represent the overall (global) stability.

To represent the retrogression process, the internal stress in the cells will gradually increase until some reach their peak stress. At this point, the stress in these cells is reduced to a residual stress, and the difference between peak and residual stress is transferred to the neighbouring cells. This reduction in stress coupled with stress re-distribution simulates the process of failure propagation and retrogression. For the purpose of the following discussion, the reduction from peak to residual stress is shown as an instantaneous process (i.e. brittle failure).

Specific failure modes (e.g. shear, tensile, compressive) have not been considered, and the forces acting between model cells, including active and passive earth pressures, have not been explicitly modelled. Instead, all of these processes are implicitly accounted for in the parameters described in the following section. The key assumption is that retrogression is driven by differences in internal pressures within the slide mass. This is approximated by a difference in the slope surface relative to the basal sliding surface, where areas that have a large deviation of the ground surface to the basal sliding surface, shown in Figure 1, will gain stress and transition to residual stress more rapidly.

The model was implemented in MATLAB.

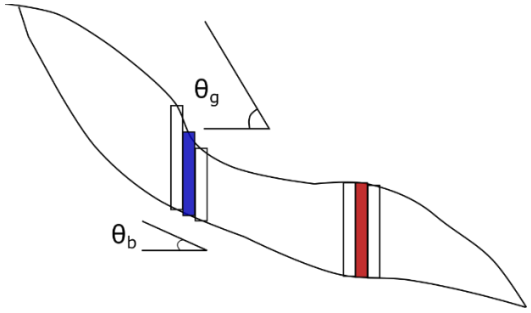

Figure 1. Schematic cross section of a landslide showing the ground surface and basal shear surface. The blue and red cells contrast a large and small relative difference, respectively, in the inclinations of the basal shear surface, θ_b, and ground surface, θ_g.

2.1 Spatial Inputs

All grids used in the model are regular square grids with equal dimensions. This discretization is shown schematically in Figure 2 in the context of the case study described in this paper. Two elevation grids are required:

one for the ground surface and one for the basal shear surface. A grid of stress increase values to be applied at each time-step is also required.

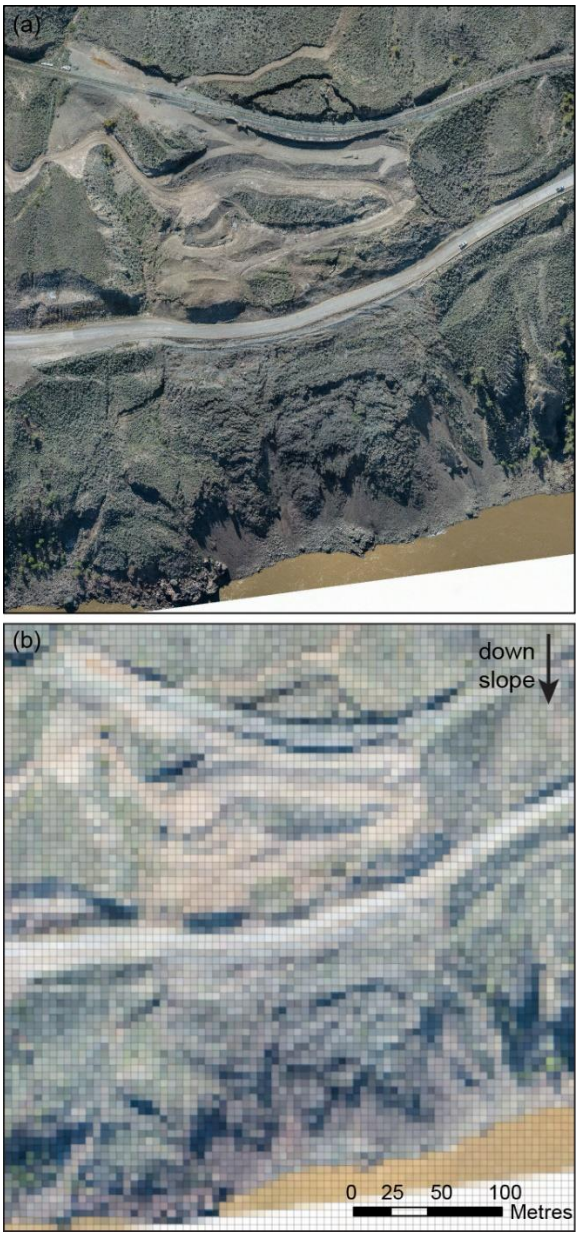

Figure 2. a) Orthophoto of Ten Mile Slide, British Columbia, from April 2017 and b) pixelated version of the photo, where each pixel represents one model cell.

The relative angle between the ground surface and basal shear surface is used in the stress calculation, detailed in Section 2.2. The ground surface and basal surface slopes, θ_g and θ_b, respectively, and aspects, α_g and α_b, respectively, shown on Figure 1, are calculated using the slope and aspect tools from the Spatial Analyst toolbox in ArcMap (ESRI 2016).

To allow for a comparison of the two angles, the ground surface slope and aspect are projected onto the vertical plane that contains the plunge and azimuth of the shear surface for that cell. The choice was made to project the ground surface onto the shear surface because the orientation of the shear surface has the greatest effect on the movement direction of landslides. The slope surface angle is projected into the same plane (aspect) as the basal surface angle using the equation for apparent dip:

$$\tan(\theta_{g,new}) = \tan(\theta_g) * |\sin(\alpha_g - \alpha_b)| \quad [1]$$

Where: $\theta_{g,new}$ is the new slope surface angle once projected onto the aspect of the basal surface plane.

The relative slope angle, θ_{rel}, represents the difference in the inclinations of the basal shear surface and the ground surface at each cell. The relative slope angle is calculated as:

$$\theta_{rel} = |\theta_{g,new} - \theta_b| \quad [2]$$

To avoid edge effects in the model a boundary is created around the edge of the active slide area, five cells wide, where the cells were allocated a relative slope of 10^{-4} to prevent them from failing. This approach allows these cells to be included as part of the analysis, but the low relative slope means that it would take a long time for them to fail.

2.2 Stress Calculation

Stresses within the model are represented by a normalized stress value, S, as shown in Figure 3. The normalized stresses must be between 0 and 1, where 1 is the peak stress of the slide material, S_p. Each cell in the model is assigned an initial random stress value, S_0.

At each time step, a stress increase is applied to each cell. The stress increase value calculated for each grid cell is a function of the relative angle between the slope and the basal shear surface, θ_{rel}, and a base value for the stress increase, S_i, as shown in Equation 3. The value of $S_i = 0.01$ was selected arbitrarily so that the maximum increase in stress on an individual cell (0.01 per time step for a cell with $\theta_{rel} = 90$ degrees) is within the same order of magnitude as the minimum increase in stress for an individual cell resulting from the stress transfer function, described in Section 2.3. Greater relative angles lead to a larger stress increase at each time step; for instance, the rate of stress increase will be greater in the blue cell than the red cell in Figure 1.

$$S_{n+1} = S_n + S_i * (\theta_{rel} / 90) \quad [3]$$

When a cell reaches its peak stress value, the cell will "yield" and drop to a residual stress, S_r. After the cell has

reached residual stress, it will remain at that constant stress.

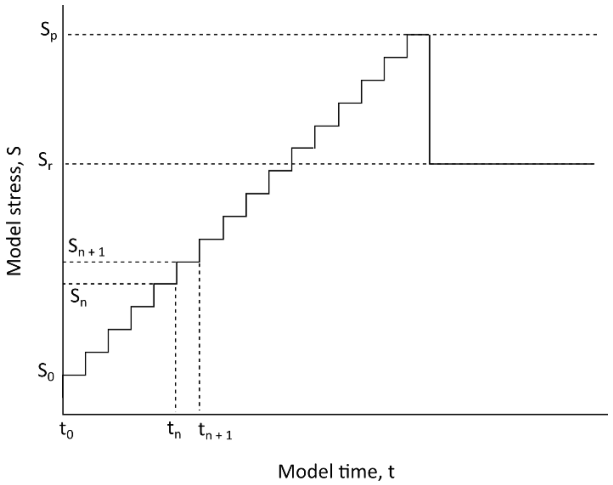

Figure 3. Conceptual stress time history for a single cell within the model where the cell reaches residual strength through the constant stress increase ($S_{n+1} – S_n$) applied at each time step ($t_{n+1} – t_n$).

2.3 Stress Transfer

The change in stress from peak to residual is distributed amongst the neighbouring cells, in an upslope and outward direction (Figure 4). This represents the arching process that has been described for soils (Terzaghi 1943).

The magnitude of stress transferred is equal to the difference between the peak and residual stress for the cell that has reached residual stress. The difference between peak and residual stress is referred to as the stress transfer increment, and is denoted ΔS. The amount of stress transferred to each neighbouring cell decreases with distance from the cell that has reached residual stress, using the exponential function shown in Equation 4.

$$\Delta S_l = l^r/\Sigma m^r \quad [4]$$

Where: ΔS_l is the stress transfer increment for layer "l", l is the layer index, increasing from the residual stress cell, m is the layer index, from 1 to n, where n is the maximum number of layers considered for the stress transfer process, and r is the rate constant in the exponential function, here set to a constant value of -1.

We have used three layers for the stress transfer, with a total of 55% of ΔS distributed to Layer 1, 27% of ΔS distributed to Layer 2, and 18% of ΔS distributed to Layer 3. Within each layer the stress transfer increment is distributed evenly amongst cells that have not reached residual stress, as shown in Equation 5.

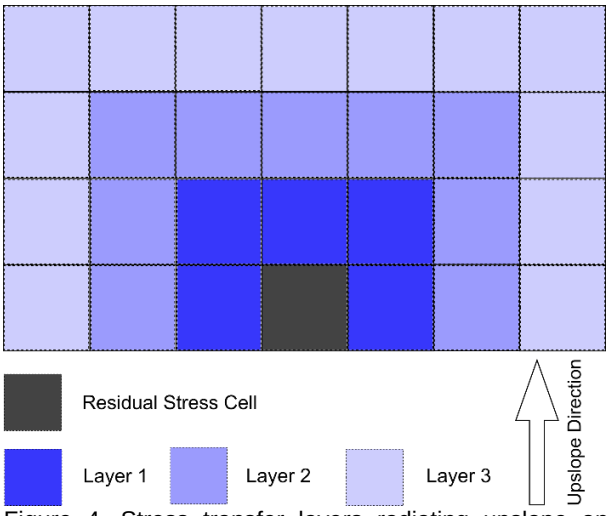

Figure 4. Stress transfer layers radiating upslope and outwards from a cell that has transitioned to residual stress.

$$\Delta S_j = \Delta S_l/p \quad [5]$$

Where: ΔS_j is the stress transfer increment for cell "j", ΔS_l is the stress transfer increment for layer "l", and p is the total number of cells not at residual stress in layer "l"

If the stress transfer process leads to one or more of the neighbouring cells reaching peak stress, the stress transfer process will continue until the stresses have transferred to cells that have not reached peak stress. At this point any neighbouring cells that have now reached peak stress will "yield", generating further stress transfer. Once all model grid cells are below peak stress the next time step of the model will begin and a new stress increase will be applied on the entire model domain, as described in Section 2.2.

3 MODEL DEMONSTRATION

An initial, proof of concept, demonstration of the model was conducted using data from Ten Mile Slide, British Columbia. A brief description of Ten Mile Slide follows, along with how the model was set up for this slide, and model results.

3.1 Ten Mile Slide, British Columbia

Ten Mile Slide is a retrogressive earth slide located at the toe of an otherwise dormant earthflow, known as the Tunnel Earthflow. Ten Mile Slide is located in the Fraser River Canyon, near the town of Lillooet in southwestern British Columbia and is affecting BC Highway 99 and a Canadian National railway line.

The landslide's geological setting and movement are described by Hensold et al. (2017). Ten Mile Slide initiated in the early 1980's, and retrogressed approximately 200 m upslope in a step-wise manner in the years up to about 2006. The slide movement is translational, following an

approximately planar basal shear surface (Hensold et al. 2017).

Surficial changes on the landslide from 2006 to 2017 have been monitored using airborne LiDAR scanning (ALS) data. Additional details on the patterns of movement within the landslide mass have been observed using terrestrial LiDAR scanning, which has shown that areas within the active slide mass move at different rates (Lato et al. 2017). The model demonstration uses data from 2006 to 2010, corresponding to a time with few anthropogenic changes to the slope. Although the area of active slope movement did not retrogress significantly in a lateral or headward direction between 2006 and 2010, slope movement rates tended to increase during this period, starting near the toe of the slide, and new areas of subsidence, bulging and ground cracking developed within the active slide mass. The model was assessed by comparing it to areas where slope damage and deformation have been observed in the LiDAR data (i.e. comparing observed tension cracks, subsidence or bulging to the areas that the model indicates are reaching residual stress).

3.2 Model Inputs

Topography obtained from an ALS survey conducted in 2006 was used for the model. A 3D surface was generated for the basal shear surface from the site investigation data described in Hensold et al (2017). A 1m x 1m grid was used for both the surface topography and shear plane. To simplify the model, and give a better demonstration of how it performs without detailed site investigation data, the basal shear surface was represented as a single plane, fitted in Cloud Compare. Using a detailed shear surface geometry that curves up to the surface can create edge effects in the stress calculation, so the simplified surface also allows a better simulation of potential retrogression.

As introduced in Section 2, specific failure modes are not considered and the stress in the model is a dimensionless value. The ratio of the tangent of the peak friction angle to the tangent of the residual friction angle, based on estimates provided in Hensold et al (2017), was used as the stress transfer increment, ΔS. A peak friction angle of 27° and a residual friction angle of 21° result in a stress transfer increment of 0.25 of peak stress in the model, which provides some physical basis for the stress transfer increment, but does not imply a rigorous application of a Mohr-Coulomb strength criteria.

The initial model run used an initial stress, S_0, corresponding to a random value between 0 and 0.1, and the value of S_i is 0.01 for all cells.

3.3 Results

The model was run up to 1000 time-steps (machine time) using the inputs described in Section 3.2. Results of this analysis are shown in Figure 5. Clusters of failed cells emerge on the steep slopes upslope of the river, near the highway level and on the highway cut slope, and on the bench directly below the rail line. These smaller clusters then begin to coalesce, forming distinct bands at residual stress in the locations mentioned above.

The model results were compared to ALS change detection results from the slide (Lato et al. 2016) to assess if the emergent behaviour of the model matched observed patterns of movement. Note that changes that occurred on the highway surface may have been obscured through regular maintenance of the road surface. Clusters of residual stress cells can also be seen upslope of the rail line, which is a location where a tension crack eventually formed.

The analysis was run with the same stress transfer inputs, but starting with the 2009 topography, shown in Figure 7. The results of this analysis were compared to ALS change detection results using topography from September 2010. This corresponds to the last ALS data collection before temporary stabilization work was started in 2011, to provide a point of comparison without significant anthropogenic changes (Gaib et al. 2012). The emergent patterns of residual stress cells in this analysis were similar to the results shown in Figure 6. An exception was that, in this case, residual stress cells were calculated in the area near the east margin, [iv] in Figure 6, earlier in the analysis. This result is likely attributed to the formation of a tension crack that is visible in the 2009 topography, leading to localized areas of steeper relative slope, in turn leading to stress concentration in this area. This demonstrates the value in updating the model with new topographic information to better refine estimates of where failures are likely to progress.

Sensitivity analyses were carried out to assess the model response to different stress transfer functions, and for different rates of transitioning from peak to residual stress. The number of layers used for the stress transfer analysis was varied from 2 to 4 to 10 layers, with the stress distributed to each layer calculated using Equation 6. The model was not found to be sensitive to this range of layers for the stress transfer. The effect of the stress transfer function was also evaluated by running the model with just the time-dependent stress increase as a function of the surface slope. In this case cells reached residual strength relatively uniformly across the steeper areas of the slope, and the coalescence of residual stress areas was not observed. The stress transfer function using the relative slope angle leads to a much better representation of observed conditions.

The sensitivity to the number of time-steps to transition from peak to residual was tested. This approximates how brittle or ductile the transition to residual stress is. The number of time-steps was varied from one (base case) to 100, as shown in Figure 8. The number of cells that are at residual stress with the initial conditions we have assumed starts to increase from zero at approximately 250 time-steps, then increases linearly as isolated areas drop to residual stress. As residual stress cells start to coalesce, the rate slopes of the curves increase rapidly, and eventually return to an approximately constant rate of cells reaching residual stress. The decrease in the overall slope of the curves with increasing time from peak to residual stress affects the rate at which failures progress in the model.

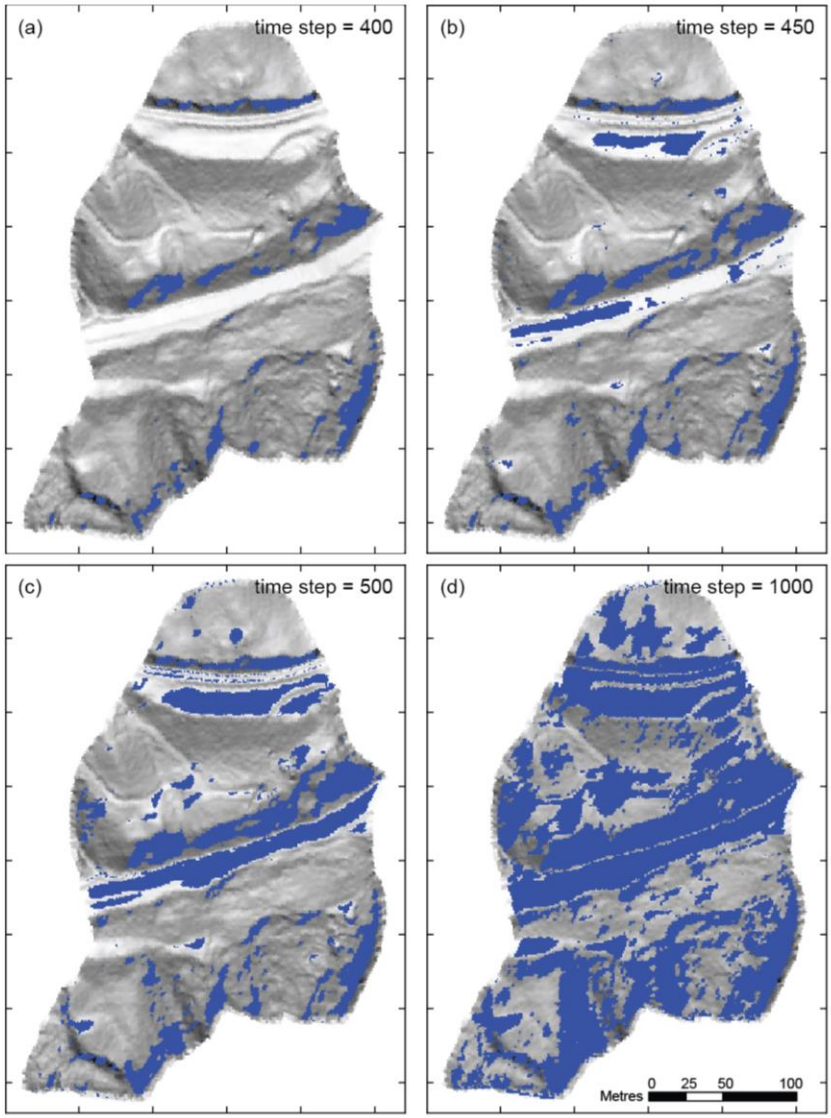

Figure 5. Model results showing: a) initial cells transitioning to residual stress (in blue), b) and c) coalescence of residual stress cells, and d) extensive areas with cells at residual stress after 1000 time-steps.

4 CONCLUSIONS AND FUTURE WORK

4.1 Application of a Cellular Model Using Data from Ten Mile Slide

We have demonstrated, at a preliminary, proof of concept level, that a simple stress transfer model implemented in a cellular model can be used to approximate the retrogression of a landslide, indicated by the emergence of areas at residual stress. The emergent behaviour of this model shows accumulations of residual stress cells in areas generally corresponding to areas of slope displacement and tension cracks measured using ALS change detection.

This cellular stress transfer model aims to represent spatial interactions over relatively limited time scales, such as the patterns of rockfalls modelled by Whadcoat (2017). The stress transfer function used in this model gives a more realistic representation of the time-dependent nature of slope damage progressing upwards and across the slope compared to an analysis of slope angle alone.

If the model is left to run long enough, the residual stress areas start to become very large, and diverge from the observations from the ALS change detection. This suggests that there is a certain time window over which the model will provide reliable results before the topography and stress conditions need to be reset.

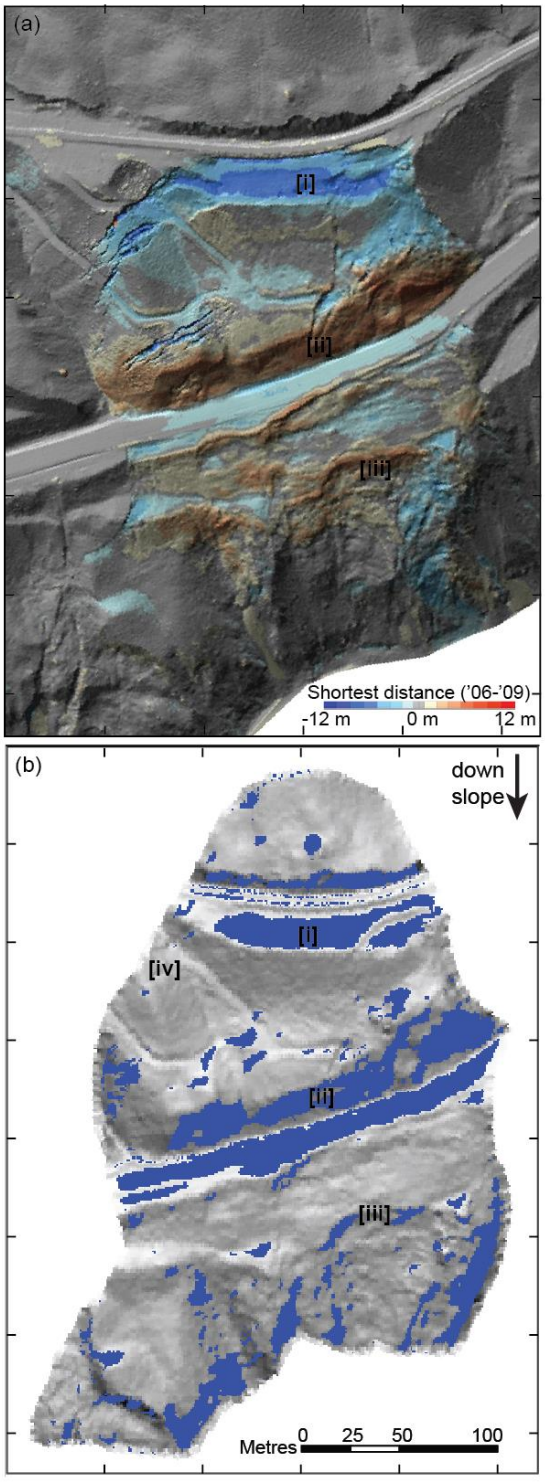

Figure 6. a) ALS change detection results from 2006 to 2009. b) Model output at 500 time-steps, with residual stress cells indicated in dark blue overlain on the hillshade surface topography. Key points indicated: [i] bench below the rail line, [ii] highway cut slope, [iii] steep slopes upslope of the river, and [iv] a steep slope on the east margin of the slide.

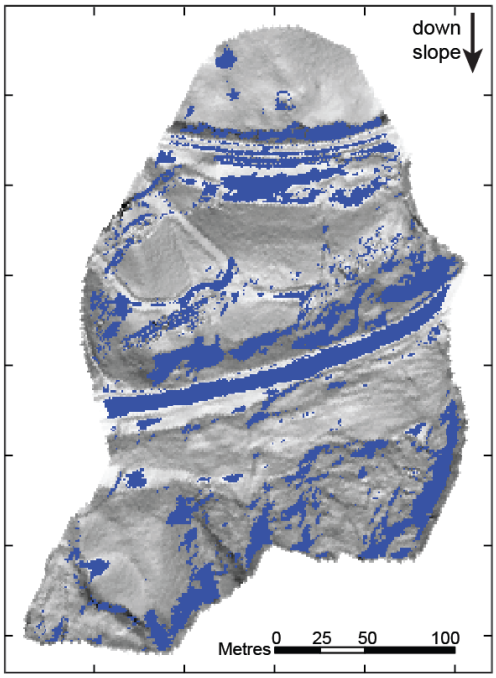

Figure 7. Model output at 500 time-steps using the topography from 2009.

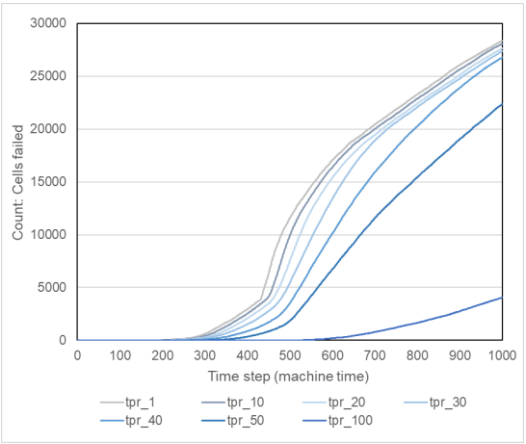

Figure 8. Sensitivity of the total number of cells that have reached residual stress for differing values of the time from peak to residual (tpr).

The stress increase function, based solely on relative slope angle, combined with the stress transfer function leads to patterns of slope damage similar to what was observed in the ALS change detection, however, there are several limitations that must be addressed before the model can be more generally applied, discussed in the following section.

4.2 Future Work

There are several limitations with the current model, and factors that can affect landslide retrogression and movement that could be explored through further

development of this model. The current model uses absolute values of relative slope angle to determine stress increase and drive failure in the model, which causes apparent damage on flatter parts of the slope, such as the highway, to emerge early in the model simulation. The timing of the modelled damage on relatively flat slopes is likely not representative of the actual failure mechanism, which should retrogress from the toe of the slope upwards, only affecting the road surface after more of the lower slope has reached residual stress. Consideration of areas that are in extensional versus compressional states within the model needs to be considered, and a more robust stress increase function needs to be developed. Additional work will be done investigating the directionality of stress transfer considering these factors.

One area of potential research that would address this issue of larger scale retrogression is to incorporate arching theory in a more detailed way, accounting for the change in the stress redistribution as clusters of residual stress cells coalesce. As the clusters become wider across the slope, the zone of peak stress would move further upslope, equivalent to the opening size in arching theory (Terzaghi 1943). The objective of this work would be to better represent the step-wise fashion in which landslides often retrogress upslope.

Incorporating downslope movements and updating the surface topography in the model without resetting the stress field would also allow for a more rigorous calibration comparing to the measured displacements. An investigation of the link between model time and real time is another area that should be investigated further when the model development moves beyond the proof of concept phase.

The effect of slope stabilization is another area of significant interest that could be investigated with a cellular model. A concern when installing stabilization measures is that the slide could transfer stress around the stabilization measures, and exploit another weak zone adjacent to the current failure, or continue to retrogress upslope and eventually overwhelm the stabilization measures.

Further testing to calibrate the model to other earthflows, or other retrogressive landslide types, would establish the general applicability of the model. The reduced complexity approach of a cellular model could also be applied to erosion related retrogressive processes, such as shoreline regression.

ACKNOWLEDGEMENTS

The authors would like to acknowledge the contributions of Matt Lato, Rod Kostaschuk, and Matthieu Sturzenegger of BGC Engineering Inc., whose work on the Ten Mile Slide stabilization project has been incorporated into this model development.

REFERENCES

Bak, P., Tang, C. and Wiesenfeld, K. 1988. Self-organized criticality, *Physical Review A,* 38: 364-374

Chapuis, A. and Tetzlaff, T. 2014. The variability of tidewater-glacier calving: origin of event-size and interval distributions, *Journal of Glaciology,* 60: 622-634

Coulthard, T.J., Hicks, D.M. and Van De Wiel, M.J. 2007. Cellular modelling of river catchments and reaches: Advantages, limitations and prospects, *Geomorphology,* 90: 192-207

Dey, R., Hawlader, B., Philips, R., and Soga, K. 2016. Numerical modeling of combined effects of upward and downward propagation of shear bands on stability of slopes with sensitive clay. *Int J Numerical and Analytical Methods in Geomechanics*, 40: 2076-2099.

ESRI. 2016. An overview of the spatial analyst toolbox. Accessed online March 8, 2018: http://desktop.arcgis.com/en/arcmap/10.3/tools/spatial-analyst-toolbox/an-overview-of-the-spatial-analyst-toolbox.htm

Gaib, S., Wilson, B., LaPointe, E. 2012. Design, construction and monitoring of an active slide area utilizing soil mixed shear keys installed using cutter soil mixing. *International Symposium on Ground Improvement IS-GI,* ISSMGE, Brussels, BE.

Hensold, G., Mitchell, A., Porter, M., Lato, M., McDougall, S., and Gaib, S. 2017. Ten Mile Slide, British Columbia: Development of a retrogressive translational earth slide in a post-glacial earthflow deposit, *3rd North American Symposium on Landslides*, AEG, Roanoke, VA, USA, 317-328.

Hergarten, S. 2003. Landslides, sandpiles, and self-organized criticality, *Natural Hazards and Earth System Science,* 3: 505-514

Hu, Q.J., Shi, R.D., Zheng, L.N., Cai, Q.J., Du, L.Q., and He, L.P. 2018. Progressive failure mechanism of a large bedding slope with a strain-softening interface. *Bull Engineering Geology and the Environment*, 77: 69-85.

Khan, Y.A., Jiang, J-C, Yamagami, T. 2002. Progressive failure analysis of slopes using non-vertical slices. *Landslides – Journal of the Japan Landslide Society*, 39(2) 203-211

Lato, M., Mitchell, A., Porter, M., and Gaib, S. 2017. Monitoring landslide velocity at Ten Mile Slide with ground-based LiDAR, *GeoOttawa 2017*, CGS, Ottawa, ON, Canada.

Leshchinsky, B., Vahedifarad, F., Koo, H-B, Kim, S-H. 2015. Yumokjeong Landslide: an investigation of progressive failure of a hillslope using the finite element method. *Landslides*, 12: 997-1005.

Liucci, L., Melelli, L., Suteanu, C. and Ponziani, F. 2017. The role of topography in the scaling distribution of landslide areas: A cellular automata modeling approach. *Geomorphology,* 290: 236-249

Piegari, E., Cataudella, V., Di Maio, R., Milano, L. and Nicodemi, M. 2006. A cellular automaton for the factor of safety field in landslides modeling, *Geophysical Research Letters,* 33: L01403

Terzaghi, K. 1943. *Theoretical soil mechanics*, John Wiley & Sons, Hoboken, NJ, USA.

Tiande, M., Chongwu, M., and Shengzhi, W. 1999. Evolution model of progressive failure of landslides. *J Geotech and Geoenv Engineering*, 125(10): 827-831.

Whadcoat, S.K. 2017. Numerical modelling of rockfall evolution in hard rock slopes: *Ph.D. Thesis,* Department of Geography, Durham University, Durham, UK, 365 p.